



# Coronary risk factors associated with OCT macrophage images and their response after CoCr everolimus-eluting stent implantation in patients with stable coronary artery disease



Yuya Taguchi <sup>a</sup>, Tomonori Itoh <sup>a,\*</sup>, Hideto Oda <sup>a</sup>, Yohei Uchimura <sup>a</sup>, Kyosuke Kaneko <sup>a</sup>, Tsubasa Sakamoto <sup>a</sup>, Iwao Goto <sup>a</sup>, Masafumi Sakuma <sup>a</sup>, Masaru Ishida <sup>a</sup>, Daisuke Terashita <sup>b</sup>, Hiromasa Otake <sup>b</sup>, Yoshihiro Morino <sup>a</sup>, Toshiro Shinke <sup>b</sup>

<sup>a</sup> Division of Cardiology, Department of Internal Medicine, Memorial Heart Center, Iwate Medical University, Japan

<sup>b</sup> Division of Cardiology, Department of Internal Medicine, Kobe University Graduate School of Medicine, Japan

## ARTICLE INFO

### Article history:

Received 10 February 2017

Received in revised form

27 July 2017

Accepted 16 August 2017

Available online 18 August 2017

### Keywords:

Optical coherence tomography

Macrophage

Coronary artery disease

Diabetes mellitus

Cobalt chromium everolimus-eluting stent

Irregular protrusion

## ABSTRACT

**Background and aims:** The aim of this study was to evaluate the accumulation of optical coherence tomography (OCT)-macrophages and OCT findings after CoCr everolimus-eluting stent placement, in addition to coronary risk factors.

**Methods:** A total of 89 lesions in 89 patients were registered in the 1- and 3-month cohort of the multi-centre study. Lesion characteristics and post-procedure OCT images were evaluated immediately and 1 and 3 months after stenting. Patients were divided into low and high macrophage grade groups based on the median macrophage grade.

**Results:** Low-density lipoprotein cholesterol (LDL-C) levels, the prevalence of diabetes mellitus, HbA1c and blood glucose levels in the high macrophage grade group were significantly higher than in the low macrophage grade group ( $p = 0.025$ ,  $p = 0.040$ ,  $p = 0.032$ , and  $p = 0.010$ ). Moreover, total lipid arc and length and number of thin-cap fibroatheromas (TCFAs) in the high macrophage grade group were significantly higher than in the low macrophage group ( $p = 0.008$ ,  $p = 0.002$ , and  $p = 0.012$ ). After CoCr everolimus-eluting stenting, there was a trend towards a greater number, height, and area of irregular protrusions in the high macrophage grade group compared to the low macrophage grade group ( $p = 0.091$ ,  $p = 0.059$ , and  $p = 0.085$ ). Multivariate logistic regression analysis showed that diabetes mellitus was a significant predictor of high macrophage grades (odds ratio: 2.8, 95% CI: 1.1–7.3,  $p = 0.030$ ).

**Conclusions:** The accumulation of OCT-macrophages was associated with diabetes mellitus in patients with coronary artery disease. Moreover, macrophage accumulation and diabetes mellitus may be associated with irregular protrusions just after stenting.

© 2017 Elsevier B.V. All rights reserved.

## 1. Introduction

Previous epidemiological studies have described several coronary risk factors [1–4]. Control of coronary risk factors is important for primary and secondary prevention in patients with coronary artery disease (CAD). Patients with CAD develop cardiac events because of acute coronary syndrome (ACS) that occurs by coronary artery occlusion caused by plaque rupture, thrombus formation and

plaque erosion [5,6]. The mechanism of ACS results in progression of the lipid core with thinning of the fibrous cap and intra-plaque inflammation [7]. The definition of vulnerable plaque described by Naghavi et al. [8] includes active inflammation in coronary plaque (invasion of monocytes, macrophages, and T-cells) and fissured plaque. Specifically, macrophages have an important role in plaque rupture of thin-cap fibroatheromas (TCFAs). Moreover, some studies have reported that induction of macrophages to plaques in patients with diabetes mellitus is more common than in patients with non-diabetes mellitus.

Recently, optical coherence tomography (OCT), which has a 10-fold higher resolution quality than that of intravascular ultrasound

\* Corresponding author. 19-1, Uchimaruru, Morioka-City, Iwate, 020-8505, Japan.  
E-mail address: [tomoitoh@iwate-med.ac.jp](mailto:tomoitoh@iwate-med.ac.jp) (T. Itoh).

(IVUS), was shown to be able not only to detect TCFA and strut coverage after stent implantation, but could also potentially evaluate macrophage invasion in coronary plaques [9].

There are several studies on the assessment of OCT-macrophages in patients with coronary artery disease. However, these studies have minimally discussed macrophage-like accumulation as visualized by OCT, coronary risk factors and in-stent response after implantation.

The purposes of this study were to assess the relationship between the intensity of the OCT-macrophage image before stent implantation and 1) clinical characteristics, including those of lesions, and 2) in-stent response (including irregular protrusions) after cobalt chromium (CoCr) everolimus-eluting stent implantation, which is a first line drug-eluting stent.

## 2. Materials and methods

### 2.1. Study patients

The MECHANISM Elective (Multicenter Comparison of Early and Late Vascular Responses to a Everolimus-Eluting Cobalt-Chromium Stent and Platelet Aggregation Studies In patients with Stable Angina Managed as Elective cases (UMINID: UMIN000012616)) study is a multi-centre registry designed to elucidate early and late vascular responses to EES for stable CAD patients using OCT. In the present study, 1 and 3-month cohorts were evaluated to elucidate early vascular responses to EES in stable CAD patients using OCT.

Target lesion characteristics were visualized by OCT. Post-procedure OCT images were evaluated immediately after stent implantation and 1 and 3 months after stent implantation of each stent. Macrophage images were defined according to the consensus of a previous report [10].

Macrophage accumulation was defined as the median macrophage grade [11]. Patients were divided into low and high macrophage grade groups.

### 2.2. Exclusion criteria

Exclusion criteria were defined as follows: clinical difficulties at a 12-month follow-up, acute myocardial infarctions, cardiogenic shock, heart failure, left main lesions, reference vessel diameters of less than 2.0 mm or more than 4.5 mm, in-stent restenosis, chronic renal failure (serum creatinine of 2.0 mg/dl), haemodialysis, cancer patients who were expected to survive for less than 2 years, elective surgeries requiring cessation of dual antiplatelet therapy, pregnant patients or scheduled pregnancies, or a prior history of allergies to aspirin or clopidogrel.

### 2.3. Definition of endpoint

Patient background characteristics were collected via an on-site registration system. Coronary risk factors were defined as hypertension, diabetes mellitus, dyslipidaemia, current smoking habits, a family history of coronary artery disease, and chronic renal failure. Diabetes mellitus was defined as blood glucose levels  $\geq 200$  mg/dl 2 h after an oral glucose tolerance test, or blood glucose levels  $\geq 200$  mg/dl, fasting glucose levels  $> 126$  mg/dl, or the presence of a prior clinical diagnosis. Dyslipidaemia was defined as total cholesterol levels  $\geq 240$  mg/dl, low-density lipoprotein cholesterol (LDL-C) levels  $\geq 140$  mg/dl, or high-density lipoprotein cholesterol (HDL-C) levels  $< 40$  mg/dl, or patients with a statin prescription. Renal insufficiency was evaluated by estimated glomerular filtration rate (e-GFR) (for Japanese patients; Japan Kidney Association). The terminal stage of renal failure was defined as e-GFR  $< 30$  ml/min/1.73 mm<sup>2</sup>, and chronic kidney disease was defined as e-GFR  $<$

60 ml/min/1.73 mm<sup>2</sup>.

### 2.4. OCT image acquisition

We performed OCT according to the Judkin's technique via the *trans*-radial or femoral approach, using a  $> 6$ -French guiding catheter system. The ILLUMIEN or ILLUMIEN OPTIS™ imaging system with the Dragonfly or Dragonfly-JP™ imaging catheter (St. Jude Medical, St. Paul, MN, USA) was used in the present study. After the insertion of a 0.36 mm intervention guide wire, the imaging catheter was carefully advanced distal to the target lesion under fluoroscopic guidance. Motorized pullback OCT imaging was performed at a pullback rate of 20 mm/s (ILLUMIEN), 18 mm/s (HD mode; ILLUMIEN OPTIS™) or 36 mm/s (ILLUMIEN OPTIS™; S mode) throughout the whole lesion. Contrast medium was flushed continuously through the guiding catheter during image acquisition. Ringer's lactate or low weight dextran fluids were available as needed because of the patient clinical conditions. Pre-dilatation using a traditional balloon  $< 2.0$  mm was approved if the pre-intervention OCT imaging catheter was not passed distally from the lesion.

### 2.5. OCT image analysis

OCT analysis was performed using LightLab OCT imaging proprietary software (LightLab Imaging/St. Jude Medical, Westford, MA, USA) by experienced observers of the Iwate Core-analysis laboratory (ICAL) as a central core laboratory staff independent of PCI. Macrophage grade images were evaluated and interpreted by discussion between two experienced and blinded observers (Y. T. and T. I). The target lesion was defined using a stent landing segment with a 5-mm addition to both the proximal and distal sides.

### 2.6. Quantitative OCT measurements

The stent area was identified in reference to a lateral branch and calcification on the OCT image after stent placement. The lumen and stent area were automatically measured using proprietary imaging software and were manually corrected by an experienced observer. Intimal thickness, mal-apposed (stent vessel distance:  $\geq 110$   $\mu$ m) and un-covered struts were evaluated using a thickness ruler according to a previous report [12].

### 2.7. Qualitative OCT measurements

The assessment of tissue properties was performed according to a previous report and consensus [10,13]. The lipid pool was defined as homogenous and diffusely bordered with signal-poor regions (Fig. 1). Lipid cap thickness was defined as the thickness of the fibrous cap covering the lipid pool. Among them, TCFAs were defined as having a thin-cap thickness of  $< 65$   $\mu$ m (Fig. 1). Plaque rupture was defined as a disrupted fibrous membrane with an underlying empty cavity. Intimal laceration was defined as the irregularity or disruption of the superficial intimal lining without fibrous cap rupture. Maximum lipid angle, maximum calcium angle, and maximum macrophage angle were measured in a target lesion around the intersection point of the largest and smallest diameters of the blood vessel lumen. Macrophage accumulation was defined as a high-intensity, signal-rich linear region with sharp attenuation (Fig. 1). Macrophage grade was defined according to previous reports [11,14], and macrophages images were classified into five groups. Macrophage signals were semi-quantitatively graded as follows: grade 0, no macrophages; grade 1, localized macrophage accumulation; grade 2, clustered accumulation in  $< 1$

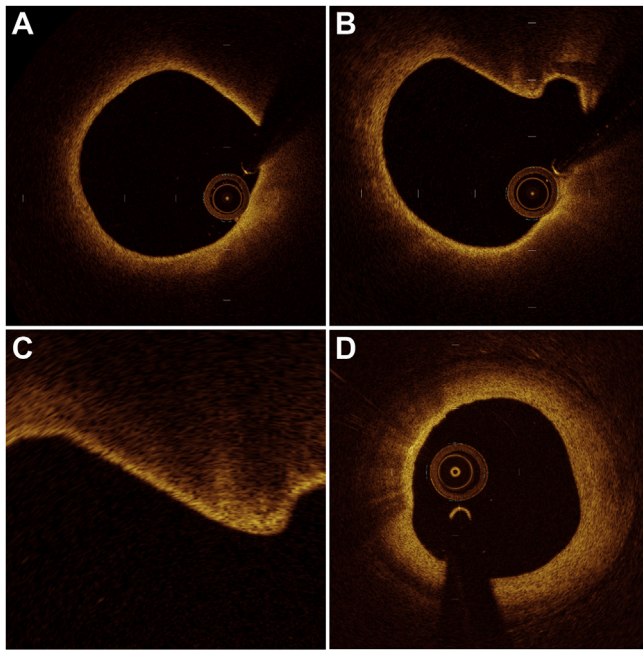


**Fig. 1.** Representative plaque images visualized by OCT.

(A) Lipid plaque: low OCT signal intensity with attenuated area and poorly delineated borders and a cap with circumference. (B) Thin cap fibro-atheroma (TCFA): low backscattering covered by a thin fibrous cap (<65  $\mu\text{m}$ ) between the vessel lumen and plaque. (C) Magnified image of B. (D) Macrophage image: macrophage accumulation was seen as confluent highly backscattering focal regions within the second quadrant of the artery wall.

quadrant; grade 3, clustered accumulation in >1 quadrant but in <3 quadrants; and grade 4, clustered accumulation in >3 quadrants. To distinguish between grades 1 and 2, the degree of macrophage extension was defined as  $30^\circ$ . Total macrophage grade was defined as the summation of macrophage grades in each cross section every 1 mm. Calcification was defined as a signal-poor or heterogeneous region with a sharply delineated border (leading, trailing, and/or lateral edges). Thrombi, irregular protrusions and prolapses were defined as abnormal in-stent tissue ( $\geq 250 \mu\text{m}$ ) [10,15]. Thrombi were also defined as a mass attached to the luminal surface or stent strut or a mass floating within the lumen. Irregular protrusion (IRP) was defined as the protrusion of material with an irregular surface into the lumen between stent struts. Prolapse was defined as a signal-rich mass with a smooth surface with low backscatter. The maximum mal-apposed area, length and number were measured at each mal-apposed area.

### 2.8. Quantitative coronary angiography

The target lesion was analysed using quantitative coronary angiography on a quantitative coronary angiography (QCA) system using the external diameter of the contrast-filled guiding catheter as the calibration standard. Minimal lumen area, lesion length, % diameter stenosis, and reference diameter were measured. Percent diameter stenosis was calculated from the minimal lumen diameter and the reference diameter. All QCA data were evaluated at the Japan Cardio-core as the central core laboratory.

### 2.9. Statistical analysis

Data are presented as the mean  $\pm$  SD. Statistical comparison of the differences in categorical data between the two groups was performed using the Chi-square contingency test. In addition,

comparison of means between the two groups was performed with a Mann-Whitney *U* test. Differences were considered statistically significant for  $p < 0.05$ . All statistical analyses were performed with SPSS for Windows, version 21.0 (Chicago, Illinois, US). Multivariate logistic regression analysis was performed with age, gender, and several coronary risk factors (hypertension, body mass index, dyslipidaemia, smoking, diabetes mellitus).

## 3. Results

### 3.1. Patient characteristics

A total of 89 lesions in 89 patients were registered in the 1 and 3-month cohort group of the present study. The median macrophage grade was 13. Patients were divided into low and the high macrophage grade groups according to their median score. Baseline patient clinical characteristics are shown in Table 1. There were no significant differences between the two groups for age, gender, or body mass index. However, LDL-C levels, the prevalence of diabetes mellitus, and the presence of elevated HbA1c and blood glucose levels in the high macrophage grade group were significantly higher than in the low macrophage grade group ( $p = 0.025$ ,  $p = 0.040$ ,  $p = 0.032$ , and  $p = 0.010$ , respectively).

### 3.2. Lesion characteristics

There were no significant differences between the high macrophage grade group and the low macrophage grade group in terms of pre-dilatation with a traditional balloon (26 (59%) vs. 22 (49%);  $p = 0.334$ ). Lesion characteristics evaluated by coronary angiography and OCT are shown in Tables 1 and 2. Although there are no significant differences between the two groups for lesion length and the number of lipid plaques, total lipid arc and length in the high macrophage grade group were significantly larger than in the low macrophage group (Fig. 2). The number of TCFAs in the high macrophage grade group was significantly higher than in the low macrophage grade group (Fig. 2).

Multivariate logistic regression analysis showed that diabetes mellitus was a significant macrophage grade predictive factor (odds ratio: 2.8, 95% CI: 1.1–7.3,  $p = 0.030$ ) and hypertension was a significant low macrophage grade predictive factor (odds ratio: 0.2, 95% CI: 0.1–0.9,  $p = 0.031$ ).

After CoCr-EES implantation, the number and total length of thrombi in the high macrophage grade group were significantly higher than in the low macrophage grade group ( $p = 0.010$ ,  $p = 0.035$ , respectively, Fig. 3). Moreover, there was a trend towards a greater number, height, and area of IRPs in the high macrophage grade group compared to the low macrophage grade group ( $p = 0.091$ ,  $p = 0.059$ , and  $p = 0.085$ , respectively, Fig. 3). There were no significant differences between the high macrophage grade group and the low macrophage grade group in regard to incidence of post-dilatation, balloon diameter, and maximum balloon pressure (Table 1).

## 4. Discussion

In the present study, macrophage grade was visualized by OCT, and patients and lesion characteristics were evaluated in patients with stable coronary artery disease. In the high macrophage grade group, LDL-C levels, the prevalence of diabetes mellitus and elevated HbA1c and blood glucose levels were significantly higher than in the low macrophage grade group. Moreover, diabetes mellitus was an independent predictor for high macrophage grades by multiple logistic regression analysis. Lipid plaque arc and length in the high macrophage grade group were significantly larger than

**Table 1**  
Baseline patient characteristics.

	High macrophage grade group (n = 44)	Low macrophage grade group (n = 45)	p-value
Age, y	71 ± 10	71 ± 8	0.928
Male gender, n (%)	30 (68)	35 (78)	0.308
Body Mass Index, kg/m <sup>2</sup>	25.0 ± 4.3	24.5 ± 3.9	0.534
Cardiovascular risk factors			
Hypertension, n (%)	34 (77)	41 (91)	0.073
Dyslipidaemia, n (%)	35 (80)	38 (84)	0.547
Diabetes, n (%)	30 (68)	21 (47)	0.040
eGFR < 60 ml/min/1.73 mm <sup>2</sup> , n (%)	16 (36)	11 (24)	0.218
Family history, n (%)	1 (2)	6 (13)	0.053
Smoking, n (%)	16 (36)	17 (38)	0.890
History			
PCI, n (%)	11 (25)	18 (40)	0.131
CABG, n (%)	0 (0)	0 (0)	N/A
AMI, n (%)	7 (16)	13 (29)	0.142
Heart failure, n (%)	5 (11)	3 (7)	0.439
Stroke, n (%)	4 (9)	5 (11)	0.752
Malignancy, n (%)	1 (2)	4 (9)	0.175
Atrial fibrillation, n (%)	6 (14)	2 (4)	0.130
COPD, n (%)	2 (5)	1 (2)	0.544
Laboratory data			
Total cholesterol, mg/dl	189.8 ± 44.0	171.8 ± 35.5	0.058
Low-density lipoprotein cholesterol, mg/dl	116.5 ± 36.8	97.2 ± 32.7	0.025
High-density lipoprotein Cholesterol, mg/dl	48.3 ± 13.9	49.6 ± 14.0	0.693
Blood glucose, mg/dl	143.1 ± 44.4	121.4 ± 36.2	0.010
HbA1c, %	6.7 ± 1.2	6.2 ± 0.8	0.032
Medication use			
Statin, n (%)	31 (70)	34 (76)	0.588
EPA, n (%)	2 (5)	2 (4)	0.982
ACE-I or ARB, n (%)	30 (68)	29 (64)	0.709
Beta-blocker, n (%)	22 (50)	16 (36)	0.168
Calcium-channel blocker, n (%)	22 (50)	23 (51)	0.917
Nitrate, n (%)	7 (16)	5 (11)	0.508
Oral hypoglycaemic agent, n (%)	22 (50)	18 (40)	0.343
Insulin, n (%)	4 (9)	0 (0)	0.038
Lesion characteristics by coronary angiography			
Culprit vessel, n (%)	20 (46)/15 (34)/9 (20)	19 (42)/16 (36)/10 (22)	0.783
LAD/RCA/LCx			
AHA/ACC lesion type, n (%)	2 (4)/9 (21)/15 (34)/18 (41)	1 (2)/6 (13)/27 (60)/11 (25)	0.110
A/B1/B2/C			
Bifurcated lesions, n (%)	14 (32)	14 (31)	0.943
Minimum lumen diameter, mm	0.87 ± 0.30	0.78 ± 0.29	0.105
Reference vessel diameter, mm	2.58 ± 0.52	2.54 ± 0.43	0.761
%DS, %	65.5 ± 11.9	69.0 ± 11.0	0.127
Stent			
Stent diameter, mm	2.9 ± 0.4	2.9 ± 0.4	0.638
Stent length, mm	24.1 ± 8.1	22.0 ± 7.2	0.270
Post balloon dilatation			
Post dilatation, n (%)	34 (77)	34 (76)	0.849
Balloon diameter, mm	3.1 ± 0.5	3.1 ± 0.4	0.961
Maximum balloon pressure, atm	15.6 ± 2.9	16.9 ± 3.3	0.152

eGFR, estimated glomerular filtration rate; PCI, percutaneous coronary intervention; CABG, coronary artery bypass grafting; AMI, acute myocardial infarction; COPD, chronic obstructive pulmonary disease; EPA, eicosapentaenoic acid; ACE-I, angiotensin converting enzyme inhibitor; ARB, angiotensin receptor antagonist; MLD, minimal lumen diameter; % DS, % diameter stenosis.

in the low macrophage grade group. The number of TCFAs in the high macrophage group was significantly higher than in the low macrophage grade group.

#### 4.1. Diabetes mellitus and macrophages

Previous reports showed a higher incidence of cardiovascular events in patients with diabetes mellitus than in patients with non-diabetes mellitus [16,17]. Previous studies demonstrated that macrophage invasion, lipid arc and length are independent predictors of plaque vulnerability in patients with diabetes mellitus [18,19]. Previous pathological studies showed that the intensity of macrophages and T-cell invasion for coronary vessel walls in patients with diabetes mellitus are significantly higher than in patients with non-diabetes mellitus [20,21]. Moreover, the increase of

macrophages was associated with necrotic core expansion, the thickness of the fibrous cap and plaque vulnerability [20]. In our present study, the high macrophage grade group showed a high prevalence of diabetes mellitus and elevated HbA1c levels and blood glucose levels (but not body mass index), indicating that diabetes may directly induce macrophage accumulation in Japanese diabetes mellitus patients, especially in patients who are not obese. Although hypertension was a significant predictive factor of low macrophage grade in multivariate analysis, the reason for this result was unclear. This result may reflect early pharmacological intervention in the study patients with hypertension.

Chia et al. [22] reported that there were no significant differences between the diabetes mellitus and non-diabetes mellitus groups in macrophage density as assessed by quantitative analysis. This could be due to the fact that the number of patients included in



**Table 2**  
Serial quantitative OCT analysis (pre and post-procedure).

	High macrophage grade group	Low macrophage grade group	p-value
<b>Pre-procedure</b>	n = 44	n = 45	
Lesion length, mm	26.0 ± 9.5	23.9 ± 11.7	0.221
Minimum lumen area, mm <sup>2</sup>	1.32 ± 0.47	1.57 ± 0.68	0.126
Lipid plaque, n	1.6 ± 0.8	1.4 ± 0.6	0.473
Total lipid arc, ° (degree)	381.0 ± 184.2	296.9 ± 117.0	0.008
Total lipid length, mm	19.3 ± 9.8	12.7 ± 7.7	0.002
No. of TCFAs, n	0.3 ± 0.6	0.1 ± 0.3	0.012
No. of thrombus, n	0.6 ± 1.1	0.4 ± 0.9	0.421
<b>Post-procedure</b>	n = 42	n = 42	
No. of thrombi, n	1.7 ± 1.9	1.0 ± 1.1	0.010
Thrombus area, mm <sup>2</sup>	0.21 ± 0.20	0.19 ± 0.23	0.306
Total thrombus length, mm	2.42 ± 2.59	1.31 ± 1.93	0.035
No. of irregular protrusions, n	0.38 ± 0.76	0.14 ± 0.42	0.091
Irregular protrusion height, mm	0.10 ± 0.17	0.03 ± 0.10	0.059
Irregular protrusion area, mm <sup>2</sup>	0.10 ± 0.21	0.04 ± 0.11	0.085
No. of mal-apposed segments, n	4.9 ± 3.1	4.1 ± 3.2	0.240
Mal-apposed area, mm <sup>2</sup>	0.37 ± 0.20	0.38 ± 0.31	0.667
Mal-apposed depth, mm	0.28 ± 0.11	0.29 ± 0.17	0.350

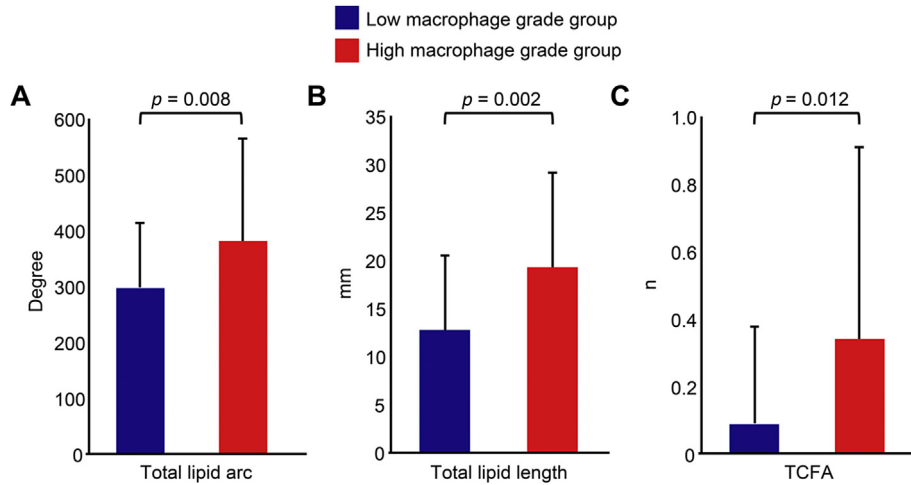


**Fig. 2.** Comparison of lipid and thin cap fibro-atheroma (TCFA) visualized by OCT between the study groups. Total lipid arc, length and TCFA (A–C) in the high macrophage grade group were significantly larger than in the low macrophage group.

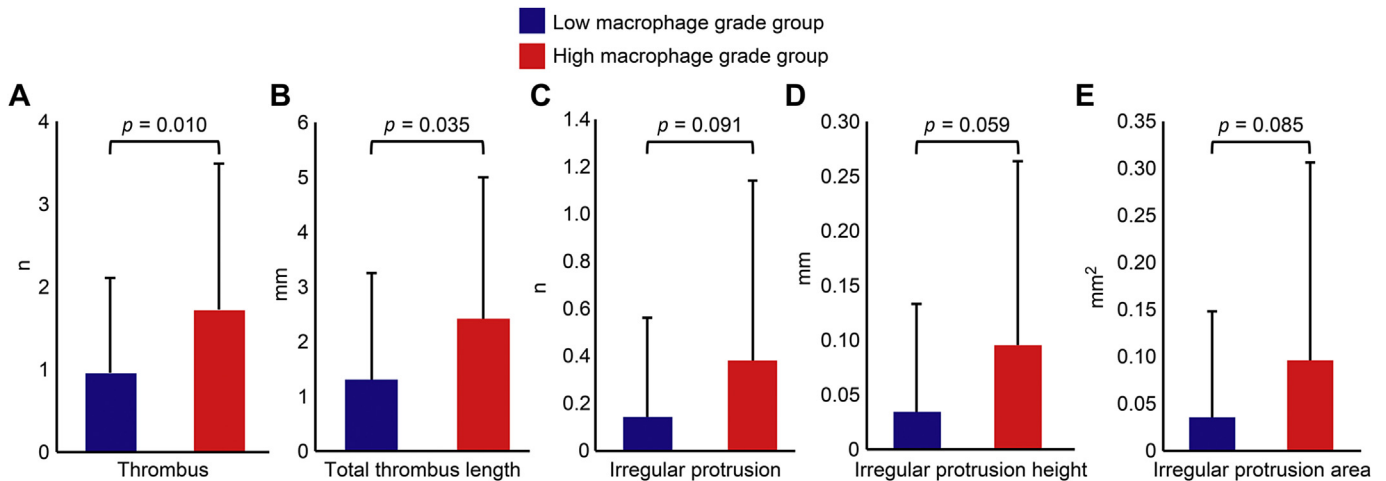


**Fig. 3.** Comparison of thrombus and irregular protrusion visualized by OCT just after stenting between the study groups. After CoCr-EES implantation, the number and total length of thrombi (A and B) in the high macrophage grade group were significantly higher than in the low macrophage grade group. Moreover, there was a trend towards a greater number, height, and area of IRPs (C–E) in the high macrophage grade group compared to the low macrophage grade group.

the study was small. Kato et al. reported plaque characteristics in triple vessel disease patients with diabetes mellitus and non-diabetes mellitus ( $n = 230$ ) [23]. They demonstrated that lipid index, calcification and the occurrence of thrombi in patients with diabetes mellitus were significantly higher than in the non-diabetes mellitus group. Moreover, lipid index, number of TCFAs and intensity of macrophage invasion in patients with poor glucose control ( $HbA1c \geq 8.0\%$ ) were significantly higher than in patients with adequate glucose control. These data support our present findings that the presence of diabetes mellitus and the degree of glucose control are associated with plaque vulnerability.

The EASY-FIT study reported that statin therapy showed an inverse correlation between the % change in macrophage grade and fibrous cap thickness, fibrous cap thickness and LDL-C levels [14]. Specifically, as macrophage grade increased, fibrous thickness decreased and LDL-C levels increased. These data support our present findings. Macrophage grades may reflect the efficacy of pharmacological intervention in patients with dyslipidaemia or diabetes mellitus. Kühnast et al. reported that treatment with a proprotein convertase subtilisin/kexin type 9 (PCSK9) inhibitor improved plaque morphology and decreased macrophage and necrotic core content in an animal model [24]. PCSK9 inhibitor treatment may improve vascular inflammation and prognosis after coronary stenting.

Vulnerable plaques, such as TCFAs, easily produce a no-reflow phenomenon and distal embolism, a higher incidence of periprocedure myocardial infarction and an insufficiency of microcirculation [25,26]. A larger lipid arc was an independent predictor of the no-reflow phenomena in this report [26]. However, macrophage grade was not assessed in this report. Although there were no significant differences in the no-reflow phenomena between the groups in our present small study, not only lipid arc but also macrophage grade may be predictors for no-reflow phenomena. Macrophage grade may be an index for the use of a distal protection device.

#### 4.2. Post-stenting findings

A previous study demonstrated that the presence of an irregular protrusion after stenting was an important predictor of long-term device oriented outcome. In the present study, the number and total length of thrombi in the high macrophage grade group were significantly higher than in the low macrophage grade group, and there was a trend towards a greater number, height, and area of IRPs in the high macrophage grade group compared to the low macrophage grade group after CoCr everolimus-eluting stenting. This result supports the hypothesis that diabetes mellitus induces macrophage accumulation and intima injury and that diabetes mellitus after stenting is associated with IRP. Moreover, IRP may be caused and reflected by the intensity of the intimal injury, and the underlying plaque characteristics, including macrophage accumulation.

#### 4.3. Study limitations

There are several study limitations in this study. First, the number of study patients was small. Further large scale studies are needed. Second, the OCT-macrophage images were evaluated by a semi-quantitative assessment. Although there have been several previous quantitative assessments of macrophages [27], this controversial problem remains. Moreover, the present study lacked pathological analysis of, and validation for macrophages. Recently, Virmani et al. reported that the OCT-macrophage image did not completely match the pathological validation findings [28]. They reported that high intensity with high attenuation correlated with

superficial macrophage accumulation in the majority of cases, but with other histological findings in 30% of cases. Sample numbers for validation were small in both studies. However, high intensity with high attenuation tissue visualized by OCT may correlate with thrombus and IRP formation without validation. Additional studies are needed to evaluate the association between clinical implications and OCT-macrophage images. Third, there are no data about plaque erosion in this study, although plaque erosion and its relationship to macrophage accumulation should be explored. Further studies are needed to evaluate the relationship between the plaque erosion and macrophage accumulation. Finally, this study was conducted as a *post hoc* analysis, and clinical prognosis after CoCr-EES stenting was not evaluated. Larger study numbers are needed in the future.

#### 4.4. Conclusion

OCT-macrophage accumulation was associated with diabetes mellitus in patients with coronary artery disease. Moreover, macrophage accumulation and diabetes mellitus may be associated with irregular protrusions after stenting.

#### Conflict of interest

Itoh T: Lecture honoraria (Daiichi Sankyo, Abbott Vascular Japan). Otake H: Lecture honoraria (Abbott Vascular Japan). Morino Y: Research grant (Daiichi Sankyo), Lecture honoraria (Daiichi Sankyo, Abbott Vascular). Shinke T: Research grant (Daiichi Sankyo), Lecture honoraria (Daiichi Sankyo, Abbott Vascular). Any other authors do not have any conflicts of interest or financial disclosures.

#### Author contributions

Yuya Taguchi: first author. Tomonori Itoh: Core labo director. Hideto Oda, Yohei Uchimura, Kyosuke Kaneko, Tsubasa Sakamoto, Iwao Goto, Masafumi Sakuma, Masaru Ishida: Core labo members. Daisuke Terashita, Hiromasa Otake: advisers. Yoshihiro Morino: principal investigator of MECHANISM-AMI study. Toshiro Shinke: principal investigator of MECHANISM-elective study.

#### Acknowledgements

The authors are deeply grateful to the core-analysis laboratory members: Kanako Omiya and Yumiko Okuyama (ARCHIMEDES (The Academic Research Group for Exploring Undiscovered Mechanisms of Cardiovascular Diseases), Kayoko Fujiwara (secretary, ICAL) and Tatsuya Shinke (image technician, ICAL).

#### Appendix A. Supplementary data

Supplementary data related to this article can be found at <http://dx.doi.org/10.1016/j.atherosclerosis.2017.08.002>.

#### References

- [1] H. Tanaka, C. Date, H. Chen, et al., A brief review of epidemiological studies on ischemic heart disease in Japan, *J. Epidemiol.* 6 (1996) S49–S59.
- [2] K. Yano, D.M. Reed, D.L. McGee, Ten-year incidence of coronary heart disease in the Honolulu Heart Program. Relationship to biologic and lifestyle characteristics, *Am. J. Epidemiol.* 119 (1984) 653–666.
- [3] D. Levy, P.W. Wilson, K.M. Anderson, et al., Stratifying the patient at risk from coronary disease: new insights from the Framingham Heart Study, *Am. Heart J.* 119 (1990) 712–717 discussion 717.
- [4] M. Kubo, Y. Kiyohara, I. Kato, et al., Trends in the incidence, mortality, and survival rate of cardiovascular disease in a Japanese community: the Hisayama study, *Stroke* 34 (2003) 2349–2354.

- [5] C.G. Santos-Gallego, B. Picatoste, J.J. Badimon, Pathophysiology of acute coronary syndrome, *Curr. Atheroscler. Rep.* 16 (2014) 401.
- [6] M.J. Davies, A.C. Thomas, Plaque fissuring—the cause of acute myocardial infarction, sudden ischaemic death, and crescendo angina, *Br. heart J.* 53 (1985) 363–373.
- [7] P. Libby, Molecular bases of the acute coronary syndromes, *Circulation* 91 (1995) 2844–2850.
- [8] M. Naghavi, P. Libby, E. Falk, et al., From vulnerable plaque to vulnerable patient: a call for new definitions and risk assessment strategies: Part I, *Circulation* 108 (2003) 1664–1672.
- [9] T. Kubo, N. Nakamura, Y. Matsuo, et al., Virtual histology intravascular ultrasound compared with optical coherence tomography for identification of thin-cap fibroatheroma, *Int. heart J.* 52 (2011) 175–179.
- [10] G.J. Tearney, E. Regar, T. Akasaka, et al., Consensus standards for acquisition, measurement, and reporting of intravascular optical coherence tomography studies: a report from the International Working Group for Intravascular Optical Coherence Tomography Standardization and Validation, *J. Am. Coll. Cardiol.* 59 (2012) 1058–1072.
- [11] S. Tahara, T. Morooka, Z. Wang, et al., Intravascular optical coherence tomography detection of atherosclerosis and inflammation in murine aorta, *Arterioscler. Thromb. Vasc. Biol.* 32 (2012) 1150–1157.
- [12] A. Konishi, T. Shinke, H. Otake, et al., Serial optical coherence tomography evaluation at 6, 12, and 24 Months after biolimus A9-eluting biodegradable polymer-coated stent implantation, *Can. J. Cardiol.* 31 (2015) 980–988.
- [13] R. Virmani, A.P. Burke, A. Farb, et al., Pathology of the vulnerable plaque, *J. Am. Coll. Cardiol.* 47 (2006) C13–C18.
- [14] K. Komukai, T. Kubo, H. Kitabata, et al., Effect of atorvastatin therapy on fibrous cap thickness in coronary atherosclerotic plaque as assessed by optical coherence tomography: the EASY-FIT study, *J. Am. Coll. Cardiol.* 64 (2014) 2207–2217.
- [15] T. Soeda, S. Uemura, S.J. Park, et al., Incidence and clinical significance of poststent optical coherence tomography findings: one-year follow-up study from a multicenter registry, *Circulation* 132 (2015) 1020–1029.
- [16] Influence of diabetes on 5-year mortality and morbidity in a randomized trial comparing CABG and PTCA in patients with multivessel disease: the Bypass Angioplasty Revascularization Investigation (BARI), *Circulation* 96 (1997) 1761–1769.
- [17] J.A. Beckman, M.A. Creager, P. Libby, Diabetes and atherosclerosis: epidemiology, pathophysiology, and management, *Jama* 287 (2002) 2570–2581.
- [18] M. Burgmaier, M. Hellmich, N. Marx, et al., A score to quantify coronary plaque vulnerability in high-risk patients with type 2 diabetes: an optical coherence tomography study, *Cardiovasc. Diabetol.* 13 (2014) 117.
- [19] S. Reith, S. Battermann, R. Hoffmann, et al., Optical coherence tomography derived differences of plaque characteristics in coronary culprit lesions between type 2 diabetic patients with and without acute coronary syndrome, Catheterization and cardiovascular interventions, official J. Soc. Cardiac Angiogr. Interventions 84 (2014) 700–707.
- [20] A.P. Burke, F.D. Kolodgie, A. Zieske, et al., Morphologic findings of coronary atherosclerotic plaques in diabetics: a postmortem study, *Arterioscler. Thromb. Vasc. Biol.* 24 (2004) 1266–1271.
- [21] P.R. Moreno, A.M. Murcia, I.F. Palacios, et al., Coronary composition and macrophage infiltration in atherectomy specimens from patients with diabetes mellitus, *Circulation* 102 (2000) 2180–2184.
- [22] S. Chia, O.C. Raffel, M. Takano, et al., Comparison of coronary plaque characteristics between diabetic and non-diabetic subjects: an in vivo optical coherence tomography study, *Diabetes Res. Clin. Pract.* 81 (2008) 155–160.
- [23] K. Kato, T. Yonetsu, S.J. Kim, et al., Comparison of nonculprit coronary plaque characteristics between patients with and without diabetes: a 3-vessel optical coherence tomography study, *JACC. Cardiovasc. Interv.* 5 (2012) 1150–1158.
- [24] S. Kuhnast, J.W. van der Hoorn, E.J. Pieterman, et al., Alirocumab inhibits atherosclerosis, improves the plaque morphology, and enhances the effects of a statin, *J. Lipid Res.* 55 (2014) 2103–2112.
- [25] Y. Ozaki, A. Tanaka, T. Tanimoto, et al., Thin-cap fibroatheroma as high-risk plaque for microvascular obstruction in patients with acute coronary syndrome, *Circ. Cardiovasc. imaging* 4 (2011) 620–627.
- [26] A. Tanaka, T. Imanishi, H. Kitabata, et al., Lipid-rich plaque and myocardial perfusion after successful stenting in patients with non-ST-segment elevation acute coronary syndrome: an optical coherence tomography study, *Eur. heart J.* 30 (2009) 1348–1355.
- [27] G.J. Tearney, H. Yabushita, S.L. Houser, et al., Quantification of macrophage content in atherosclerotic plaques by optical coherence tomography, *Circulation* 107 (2003) 113–119.
- [28] C. Lutter, H. Mori, K. Yahagi, et al., Histopathological differential diagnosis of optical coherence tomographic image interpretation after stenting, *JACC. Cardiovasc. Interv.* 9 (2016) 2511–2523.